Paving the Way for K-ion Batteries: Role of the Electrolyte Reactivity Through the Example of Sb-based Electrodes

Lénaïc Madec[1,4,], Vincent Gabaudan[2,4], Grégory Gachot[3,4], Lorenzo Stievano[2,4], Laure Monconduit[2,4], Hervé Martinez[1,4]*

[1] CNRS/ UNIV Pau & Pays Adour/ E2S UPPA, Institut des Sciences Analytiques et de Physicochimie pour l'Environnement et les Matériaux, UMR5254, 64000, Pau, France

[2] ICG-AIME, Bat 15, cc 15-02, Université Montpellier 2, Pl. E. Bataillon, 34095 Montpellier cedex 5, France

[3] Laboratoire de Réactivité et Chimie des Solide (LRCS), CNRS, UMR 7314, Université de Picardie Jules Verne, 33 rue Saint Leu, Amiens, France

[4] Réseau sur le Stockage Electrochimique de l'Energie (RS2E), CNRS FR3459, 33 Rue Saint Leu, 80039 Amiens Cedex, France

KEYWORDS. Potassium-ion, electrolyte, interaction, XPS, GC/MS

ABSTRACT. Developing potassium-ion batteries remains a challenge so far due to the lack of efficient electrolytes. Moreover, the high reactivity of K metal and the use of half-cells may greatly alter both the electrochemical performance and the solid electrolyte interphase formation. Here, it is showed that, in K metal/Sb half-cells, coulombic efficiency improvement is achieved by the addition of FEC + VC to PC, the replacement of PC by EC:DEC and the replacement of KPF_6 by KFSI. Surprisingly, however, storage of cells containing K metal leads to the coloration of K metal, separators and Sb electrodes, whereas no change occurs for cells prepared without K metal. These results demonstrate that for all electrolytes, the high electrolyte reactivity with K metal also influences the Sb/electrolyte interface via a cross-talk mechanism. This observation is supported by GC/MS analysis of electrolytes and XPS analysis of Sb electrodes. In summary, these results indicate that the search for efficient electrolytes for KIBs must be carried out in full cells if one wants to obtain meaningful correlations between electrochemical performance and electrode/electrolyte interfaces properties. Overall, the results presented here are also likely to benefit to the development of other emerging Na, Mg-ion cell chemistries.

1. Introduction

Potassium ion batteries (KIBs) are foreseen as a promising alternative large-scale energy storage system of intermittent energy sources thanks to the K abundance (2.09 wt.% of the Earth's crust) and cell voltage. Indeed, beyond aqueous K-ion batteries[1], when nonaqueous electrolytes such as propylene carbonate (PC) are used, the K^+/K couple offers the lowest redox potential with -2.88 V vs. SHE compared to Li^+/Li (-2.79 V) and Na^+/Na (-2.56 V).[2] From the energy density perspective, such wider voltage operation of KIBs is therefore expected to advantageously compensate for the heavier atomic mass (39.10 g mol^{-1}) and larger ion radius (1.38 Å) of K^+

compared to Li^+ (6.94 g mol^{-1}, 0.76 Å) and Na^+ (22.99 g mol^{-1}, 1.02 Å).[3] Moreover, the lower charge density of K^+ results in smaller solvated ions, therefore offering enhanced ionic transport properties in bulk electrolytes and at the electrode/electrolyte interfaces.[4] For these reasons, the development of new materials for KIBs has recently received a growing interest.[5,6]

However, research on suitable and efficient electrolytes for KIBs has remained a challenge so far. Indeed, most of the studies on KIBs rely on the use of K metal half-cells for which the highly reactive potassium greatly alter both electrochemical performance and interphase formation. For instance, the use of 1M KFSI EC:DEC (1:1 in volume) electrolyte was found beneficial to the cycling of the Bi anode material[7] while it was found detrimental in the case of the $K_{1.6}Mn[Fe(CN)_6]_{0.96}\bullet 0.27H_2O$ cathode material.[8] The latter was explained by the formation of a highly passivating solid electrolyte interface (SEI[9]) and dendrites at the K electrode surface.[8] More generally, the replacement of KPF_6 by KFSI as electrolyte salt was found to be beneficial to the half-cells cycling of most of the anode materials[7,10,11] but it remains to be investigated in the case of cathode materials. Moreover, glyme-based electrolytes have been showed to improve electrochemical performance compared to carbonate-based electrolyte due to a better wettability of the electrodes.[10,12] Interestingly, a glyme-based (DME) electrolyte combined with the KFSI salt was also reported to enable highly reversible potassium plating/stripping due to the formation of uniform SEI compared to carbonate-based and KFP_6-based electrolytes.[13] Overall, beyond the lifetime and safety concerns, these literature reports clearly highlight the limit and complexity of using K-ion half-cells. Moreover, the reactive potassium is expected to dramatically increase interactions (cross-talk) between electrodes that have been commonly reported for Li-ion cells.[14,15,16,17,18,19] Therefore, the in-depth investigation of the electrolytes impacts on both

electrochemical performance and electrode/electrolyte interface formation, appears of great interest for the further development of KIBs.

The present paper thus focuses on the study of the electrolyte reactivity in K metal/Sb half-cells and its impact on the electrode/electrolyte interfaces formation. The electrolyte composition is tuned by varying both solvents and salts to improve the coulombic efficiency during the first cycle. For the first time, gas chromatography coupled with electron impact mass spectrometry (GC/MS) and X-ray photoelectron spectroscopy (XPS) analyses are combined to investigate any possible interaction (cross-talk) via the migration of electrolyte degradation species from the K metal to the Sb electrode.

2. Experimental

2.1. Cell preparation and cycling protocol. Electrodes were prepared by mixing Sb powder (~325 mesh, 99.5% purity, Alfa-Aesar), carbon black (C65, BET = 65 m^2 g^{-1}, Timcal), vapor ground carbon fibers (VGCF-S, BET = 15 m^2 g^{-1}, Showa Denko) and carboxymethyl cellulose (CMC, DS = 0.7, Mw = 250 000, Aldrich) with a 70:9:9:12 weight ratio in deionized water (0.8 ml) using a silicon nitride vial and a planetary ball-milling for 1 h. The obtained slurry was then tape casted on a 17.5 µm thick copper foil (99.9 %, Goodfellow) with a 150 µm thickness and dried for 24 h at room temperature. Electrodes with 12.7 mm diameter were then punched out and dried for another 12 h at 80 °C under dynamic vacuum. The final active material loading of the electrode was 2 mg cm^{-2} ± 0.3 mg.

Propylene carbonate (PC, anhydrous, 99.7% purity), diethyl carbonate (DEC, anhydrous, ≥99% purity), 1,2-dimethoxyethane (DME, anhydrous, 99.5% purity, inhibitor-free), diethylene glycol dimethyl ether (diglyme, anhydrous, 99.5% purity) and vinylene carbonate (VC, 80 ppm BHT as

stabilizer, 99% purity) were purchased from Aldrich. Ethylene carbonate (EC, anhydrous, 99% purity) and fluoroethylene carbonate (FEC, 98% purity) was purchased from Alfa Aesar. Potassium hexafluorophosphate (KPF_6, 99% purity) and potassium bis(fluorosulfonyl)imide (KFSI, 99.9% purity) were purchased from Aldrich and Solvionic, respectively. 1M KPF_6 PC, 1M KPF_6 PC + 5% FEC + 1% VC (in wt.%), 0.8M KPF_6 EC:DEC, 0.8M KFSI EC:DEC, 1M KPF_6 DME and 1M KPF_6 diglyme electrolytes were prepared. In an argon-filled glove box, 2032 coin cells were assembled using Sb-based electrodes, a glass-fiber paper (GF/D, Whatman) and a polypropylene-polyethylene-polypropylene membrane (Celgard) as separators without or with a potassium foil (from Aldrich), all soaked in 200 µl of electrolyte.

Storage experiments were performed for cell assembled with or without K metal for 3 weeks at 25°C in open-circuit conditions. Note that when K metal was used, the K metal electrode was purposely undersized following some previous work on Li-metal half-cells [20] in order to visually observe any possible change occurring at the Sb electrodes.

Electrochemical cycling was performed using an MPG battery cycler (Biologic SA, France) between 0.005-2 V at C/10 (for electrochemical performance) or C/5 (for XPS analysis) rate (*i.e.* 0.1 or 0.2 mole of K per mole of Sb per hour) and 25 ± 1 °C. At least two identical coin cells were prepared for reproducibility. After either storage or cycling, coin cells were opened under argon and Sb-based electrodes were washed twice by immersion during 10 s in a glass vial containing 0.8 ml of the electrolyte solvent used in the cell.

2.2. Gas Chromatography Coupled with Electron Impact Mass Spectrometry (GC/MS). GC/MS was performed using a TRACE™ 1300 GC ultra gas chromatograph equipped with a BPX70 cyanopropyl polysilene-siloxane based capillary column (30 m × 0.25 mm i.d., 0.25 µm)

from SGE. Helium was used as the GC carrier gas with a constant 1.3 mL/min flow rate. To achieve good chromatographic peaks resolution, the temperature gradient was optimized as follows: the capillary column was ramped from the initial 40°C temperature, held for 5 min, increased by 10 °C/min up to 250 °C and held for 10 min. The transfer line was maintained at 250 °C. The ion source was set at 200 °C. The GC was interfaced with an ISQ mass spectrometer (Thermo Scientific). Tuning of the mass spectrometer was done automatically using the ions resulting from perfluorotributylamine ionization. The mass spectrometer was operated with a 250 μA filament current of and a 70 eV electron energy in the electron ionization (EI) mode. The mass range was 10-300 u and data acquisition/processing were performed with Xcalibur 2.0.7 software. Compounds identification and corresponding structural formulae were assigned using the National Institutes of Standards (NIST) library.

2.3. X-ray Photoelectron Spectroscopy (XPS). XPS was performed using an Escalab 250 Xi spectrometer using a monochromatized Al Kα radiation (hν =1486.6 eV). Electrode samples were put on a sample holder using an insulating uPVC tape (reference 655 from 3M) then the samples transfer was performed through an argon-filled glove box directly connected to the spectrometer. Before analysis, samples were kept at 10^{-8} mbar for one night. Analysis was performed using the standard charge compensation mode and an elliptic 450 x 900 μm X-ray beam spot. Core spectra were recorded using a 20 eV constant pass energy with a 0.15 eV step size and short time iterative scans. Using CasaXPS software, the binding energy scale was calibrated from the 285 eV peak (C-C/C-H). A non-linear Shirley-type background [21] was used for core peaks analysis while 70% Gaussian - 30% Lorentzian Voigt peak shapes and full width at half-maximum constraint ranges

were selected to optimize areas and peak positions. XPS quantification were performed using the relative sensitivity factors provided with the Escalab machine.

3. Results and discussion

3.1. Electrochemical performance

Figure 1 shows the cell potential versus capacity (mAh/g_{Sb}) and coulombic efficiency (CE) for the first cycle between 0.005-2 V at C/10 and 25 ± 1 °C for Sb/K coin cells filled with different electrolytes as indicated. Overall, the galvanostatic discharge curves showed the expected shape corresponding to the electrochemical alloying process of Sb with K to form K_3Sb,[22] although some discrepancies (such as a variable polarization) are observed as function of the electrolyte. In all cases, the first discharge capacity was significantly higher than the theoretical one (660 mAh g^{-1}_{Sb}) indicating the formation of SEI films. However, only carbonate-based electrolytes allowed the following reversible charge processes, whereas glyme-based electrolytes showed systematic failures more likely due to internal short-circuiting induced by K dendrites formation.[8] Among carbonate-based electrolytes, the CE was significantly increased by the addition of FEC + VC to PC, the replacement of PC by EC:DEC and the replacement of KPF_6 by KFSI. The worst CE was therefore observed for 1M KPF_6 PC (59%) while the highest CE was observed in the case of 0.8M KFSI EC:DEC (84%). Note that beyond the increase of CE, the replacement of KPF_6 by KFSI also led to a higher polarization. This result is explained by the formation of more passivating (*i.e*. more resistive) SEI films at the K and/or Sb electrodes surface due to the KFSI salt. Indeed, the CE was further increased in the next few cycles and reached relatively stable values around 94-99% with KFSI (Figure S1b). At the opposite, no stabilization and a huge CE decrease (down to around 40%) was observed in the case of KPF_6 (Figure S1b) more likely due to continuous and large

electrolyte degradation. This agrees well with the relatively stable capacity retention observed during the corresponding 25 cycles with KFSI while the use of KPF_6 led to a drastic capacity decrease after only 10 cycles (Figure S1a). Note also a peculiar feature around 1.5 V in charge for all cells cycled in carbonate-based electrolytes. This feature, much more pronounced with the use of EC:DEC, remains, however, unclear at this point as it is not observed in following cycles (not shown).

At this point, considering the well-known high reactivity of K metal, the increase of the CE could originate from the formation of a more stable and/or passivating SEI at the K surface rather than at the Sb electrode surface. In any case, tuning the electrolyte composition appears of great importance for KIBs to obtain meaningful electrochemical data.

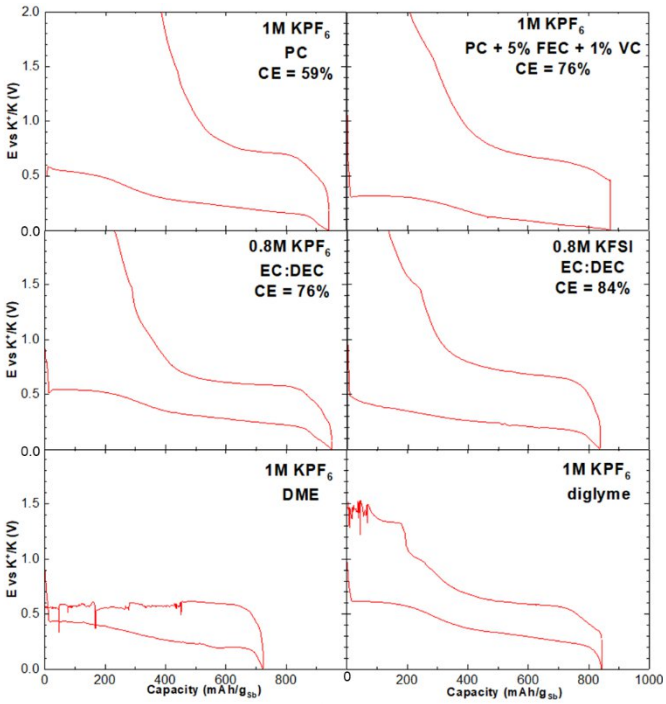

Figure 1. Cell potential versus capacity (mAh g^{-1}_{Sb}) and coulombic efficiency (CE) for the first cycle between 0.005-2 V at C/10 and 25 ± 1 °C for Sb/K coin cells filled with different electrolytes as indicated. Galvanostatic curve for only one cell is presented for better clarity.

3.2. Electrolyte reactivity

To evaluate the electrolyte reactivity, coin cells were first opened and visually inspected (Figure 2). GC/MS on the extracted electrolyte and XPS on the Sb electrodes were also performed.

3.2.1. Visual inspection. When the stored cell did not contain K metal, no coloration change of the separators, nor of the Sb electrodes was observed, independently of the electrolyte nature (not showed). This suggests a very low reactivity of all tested electrolytes with Sb electrodes. This was further confirmed by GC/MS and XPS analysis for which almost no change was observed (Figure S2-S3).

When the stored cells contained K metal, however, significant changes occurred as observed on the photographs of the potassium electrodes, separators and Sb electrodes (Figure 2). For carbonate-based electrolytes, the potassium turned ‘’blue’’. Moreover, the separator became ‘’brown’’ with PC while no change was observed with EC:DEC. At the opposite, no change was observed by GC/MS with PC while a reduction product of DEC was detected with EC:DEC (Figure S1). Note also that FEC was fully consumed for 1M KPF_6 PC + 5% FEC + 1% VC (Figure S1), further highlighting the high reactivity of K metal. In the case of DME- and diglyme-based electrolytes, potassium turned ‘’gray’’ and ‘’yellow’’, respectively. Moreover, the separator was ‘’yellow’’ with diglyme while no change was observed with DME. These results therefore highlight a completely different reactivity of the potassium with glyme-based electrolytes.

Overall, for all electrolytes, the observed separator coloration occurred mostly on the side in contact with the K metal electrode (Figure 2) due to the high reactivity of the potassium, which highlights the formation of species that diffuse in the bulk electrolyte. This result is of high importance as it implies the occurrence of interactions (cross-talk) between electrodes. As a matter of fact, in the case of EC:DEC based electrolytes (Figure 2), non-uniform Sb electrodes with two distinct regions were observed. The Sb regions superimposed to the K metal showed a different color than the rest of the Sb electrode surface. This observation can only be explained by the migration of electrolyte degradation species from K metal to the superimposed part of the Sb electrode.[20] Moreover, this phenomenon was the most pronounced in the case of 0.8M KFSI EC:DEC electrolyte, which also showed the highest CE (Figure 1). At this point it is therefore difficult to conclude whether the higher CE originates from the formation of a more efficient SEI at the K surface or at the Sb electrode surface or at both electrodes surface. In any case, it clearly highlights the challenge of using half-cells to study electrolyte impact in KIBs.

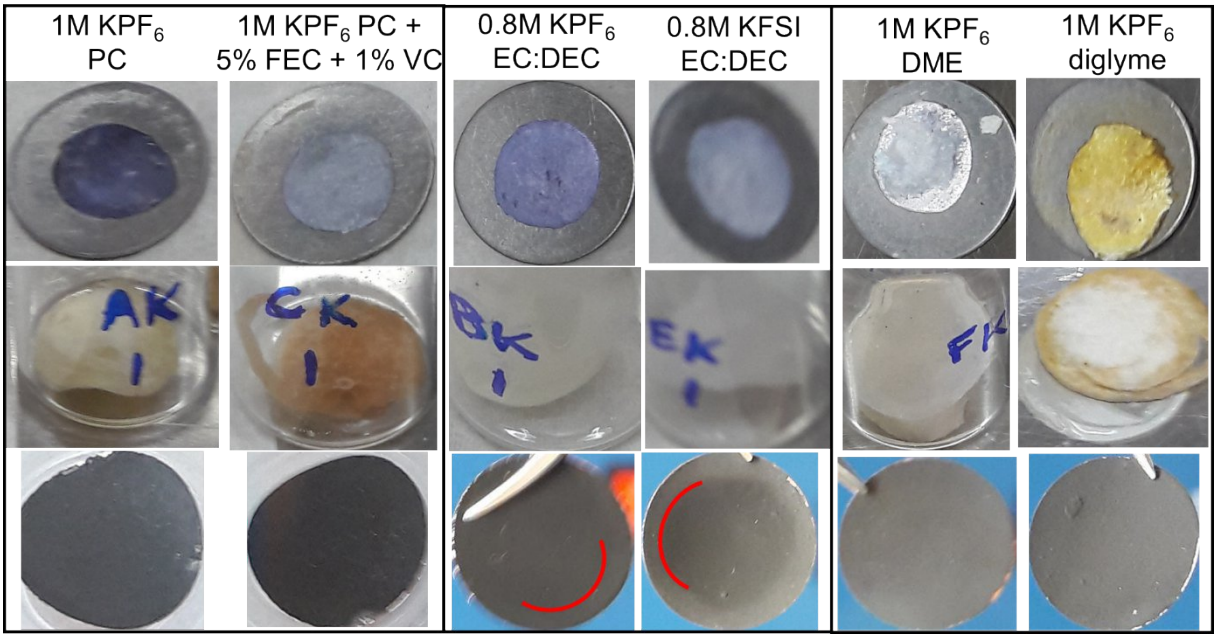

Figure 2. Photographs of the potassium electrodes, separators and Sb electrodes after storage for 3 weeks at 25 °C in coin cells with K metal and filled with different electrolytes as indicated. Only one cell is showed for clarity. Note that K metal electrodes were purposely undersized for storage experiments so that if significant changes have occurred, they could have been visually observed. Photographs are thus presented with respect to the real scale.

3.2.2. XPS analysis. Figure 3 shows the a) Carbon 1s - Potassium 2p and b) Oxygen 1s - Antimony 3d XPS core spectra of the fresh Sb electrode, Sb electrodes after storage for 3 weeks in coin cells without and with K metal and Sb electrodes after one cycle (at 2V) at C/5 and 25°C for the 0.8M KPF_6 EC:DEC and 0.8M KFSI EC:DEC electrolytes. In Figure 3, the core level spectra of the fresh Sb electrode were maximized to show low intensity peaks while for stored/cycled Sb electrodes, core level spectra for a given element were normalized to allow a direct comparison of the relative intensity/amount of the given element between samples.[19,23]

The C 1s spectrum of fresh Sb electrode showed seven components at 284.5 (C=C), 285.0 (C-C, C-H), 286.0 (-CO), 287.3 (-CO from CMC), 288.6 ($-CO_2$), 290.1 ($-CO_3$) and 291.3 eV (‘’shake up’’ satellite) from the carbon additives [24,25] and CMC binder.[26] The O 1s spectrum of fresh Sb electrode showed three peaks at 530.3, 531.6 and 533.1 eV from Sb oxide layer at the Sb surface,[27] $-CO_2$/$-CO_3$ and -CO from the carbon additives and CMC binder, respectively.[26,28] The Sb 3d spectrum of fresh Sb electrode showed two doublets at 528.5–537.9 and 530.4–539.8 eV assigned to metallic Sb and Sb oxide layer from the Sb material. An additional peak was also observed at 535.7 eV due to Na Auger from the CMC binder [27].

After storage without K metal, very small amounts of K-based species (typically < 5 At.%) were observed with the appearance of K doublets at ~293.4 and ~296.2 eV (i.e. K $2p_{3/2}$ and $2p_{1/2}$ peaks)

due to a relatively low degradation of both KPF_6 and KFSI salts (Figure 3 for EC:DEC based electrolytes and Figure S3 for the other electrolytes). This result is in agreement with the relatively low intensity decrease of the C=C (from carbon additives) and Sb peaks due to the covering by salts F-, P-, N- and S-containing salt degradation (Table S1). Overall, independently of the electrolyte nature, no significant change occurred for storage without K metal, indicating a very low reactivity of Sb electrodes with all tested electrolytes. After storage with K metal, however, significant changes occurred. For instance, much larger amounts of K-based species (~293.4-296.2 eV) and large amount of additional -CO (~533.4 eV), $-CO_2$/$-CO_3$/SO_x (~531.8 eV) based species were observed, due to both salts and solvent degradation (Figure 3 for EC:DEC based electrolytes and Figure S4 for the other electrolytes). This result is in agreement with the high intensity decrease of the C=C (from carbon additives), Sb and Na Auger peaks due to the covering by SEI films (Figure 3 and S4). Note that for the 0.8M KFSI EC:DEC electrolyte, a unidentified Sb-based species was observed (see yellow peak in Figure 3). Overall, independently of the electrolyte nature, significant change occurred at the Sb electrode for stored cells containing K metal. This result therefore clearly highlights the occurrence of interactions (cross-talk) between electrodes by migration of electrolyte degradation species from the K to the Sb electrode for all tested electrolytes, in agreement with the visual inspection discussed previously (Figure 2). After one cycle at 2V, both 0.8M KPF_6 EC:DEC and 0.8M KFSI EC:DEC electrolytes showed similar salts and solvent degradation species but with different ratios (Figure 3). Thicker SEI films were also observed after one cycle as the C=C (from carbon additives), Sb and Na Auger peaks were significantly decreased (Figure 3 and Table S1). An inhomogeneous covering, however, was observed after one cycle as Sb was not visible anymore while the carbon additives and CMC were still visible, indicating a specific reactivity of the Sb elements towards the electrolytes.

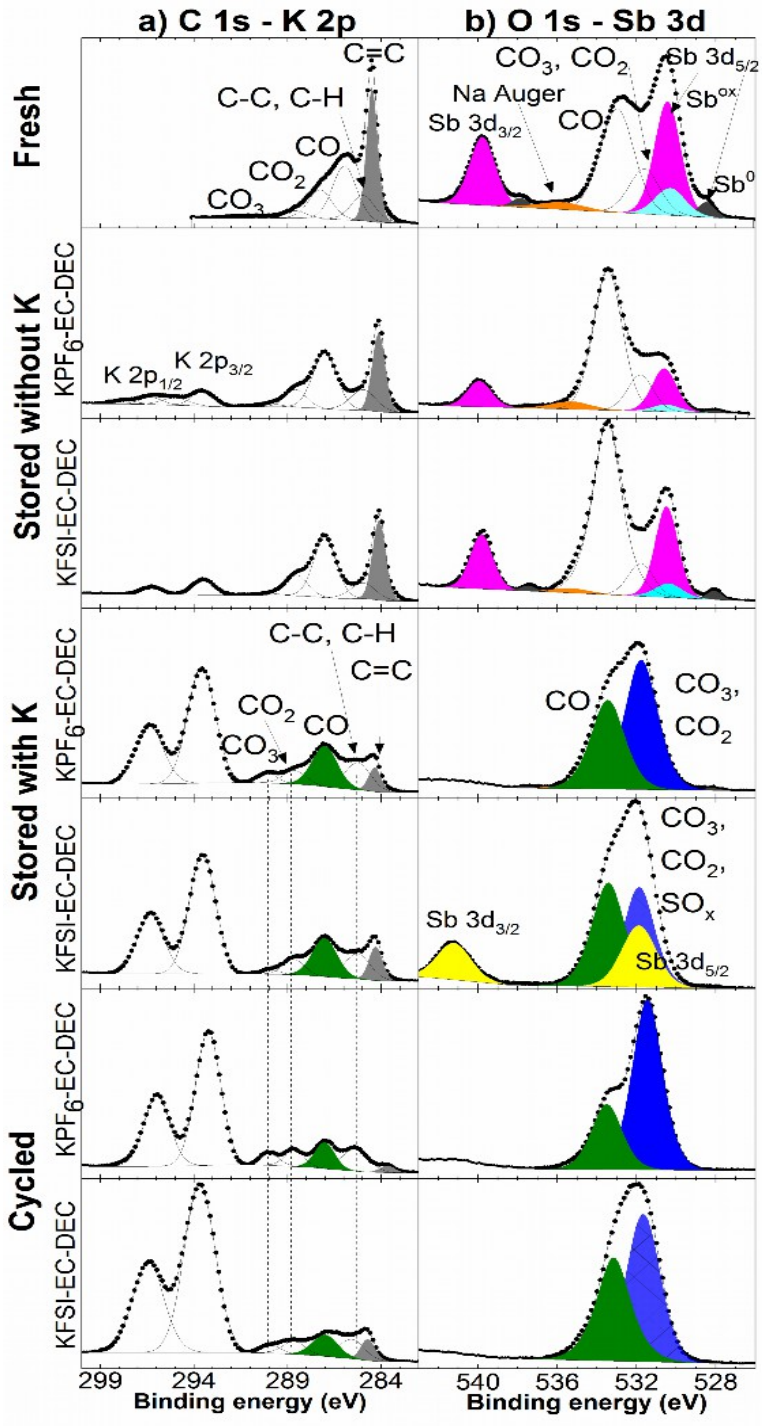

Figure 3. a) Carbon 1s - Potassium 2p and b) Oxygen 1s - Antimony 3d XPS core spectra of the fresh Sb electrode, Sb electrodes after storage for 3 weeks at 25 °C in coin cells without and with

K metal and Sb electrodes after one cycle between 0.005-2 V at C/5 and 25 °C for the 0.8M KPF_6 EC:DEC and 0.8M KFSI EC:DEC electrolytes.

Overall, even considering the high reactivity of the K metal with the electrolyte, and the migration of the reacted species to the Sb electrode, it remains difficult to provide more detailed information about the chemical nature of the SEI films formed at the Sb electrode.

Figure 4 summarizes the main SEI characteristics trends observed from the XPS quantification (Table S1) of Sb electrodes stored with K metal for all electrolytes. It should be therefore kept in mind that the SEI features discussed thereafter arise from the migration of electrolyte degradation species from the K metal to the Sb electrode. When using PC, a much lower content of salt-based species was observed with the addition of FEC and VC as additives which indicates their preferential reaction at the potassium surface, in agreement with both the higher CE (Figure 1) for the first cycle and the full consumption of FEC (Figure S2). Interestingly, for EC:DEC, the replacement of KPF_6 by KFSI led to a higher salt-based species content which cover preferentially Sb than CMC or C additives which may be related to the higher CE previously observed (Figure 1). More generally, except for 1M KFSI EC:DEC, the higher the salt-based species content was, the higher both Sb and CMC covering were. This indicates a preferential and similar covering of both the Sb active material and CMC binder by the salt-based species. No trend can be observed, however, between the salt-based species content and the carbon covering.

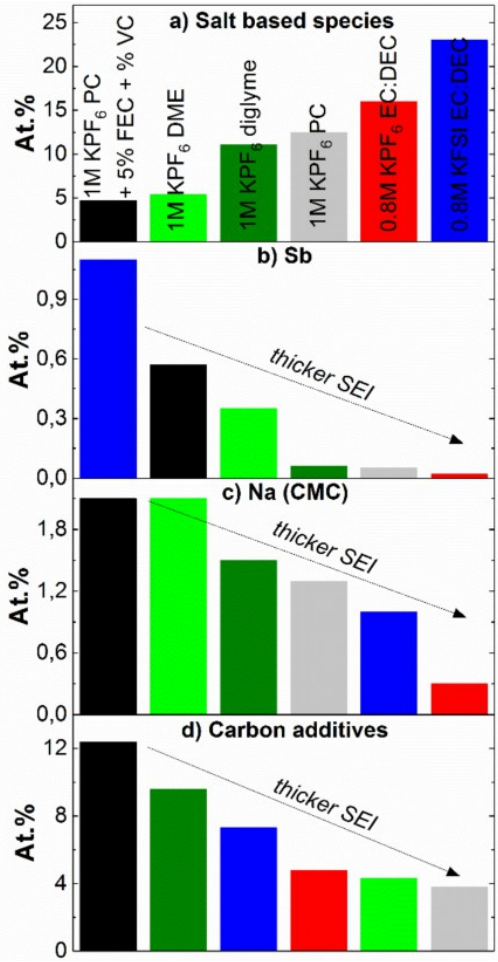

Figure 4. Atomic percent of a) salt-based species (i.e. sum of F, P, N, S and K at.%), b) Sb, c) Na (from CMC) and d) carbon additives for Sb electrodes stored for 3 weeks in coin cells containing K metal and filled with different electrolytes as indicated.

4. Conclusion

In this paper, the impact of the electrolyte reactivity in K metal/Sb half-cells on the formation of the electrode/electrolyte interface was investigated. For all studied electrolytes, galvanostatic discharge curves corresponding to the formation of the K_3Sb phase were observed. However, only carbonate-based electrolytes allowed the following reversible charge process, whereas glyme-based electrolytes showed systematic failures. The coulombic efficiency was significantly

improved by the addition of FEC + VC to PC, the replacement of PC by EC:DEC and the replacement of KPF_6 by KFSI. Visual observation performed on separators/Sb electrodes after storage without K metal showed no change while after storage with K metal, significant changes occurred such as the coloration of the K metal, coloration of the separators and different colorations of a given Sb electrode. Beyond the highlighting of the well-known high reactivity of K metal, these results clearly demonstrate the occurrence of interactions (cross-talk) between electrodes with the migration of species from the K to the Sb electrodes in all studied electrolytes. This was further confirmed by GC/MS of the electrolytes and in depth XPS analysis of the SEI films formed at the Sb electrodes surface. Therefore, despite that some SEI characteristics trends have been extracted for the different electrolytes, it remains difficult to fully understand the exact nature of the SEI films formed at the Sb surface and to correlate it to the electrochemical performance. Indeed, the origin of the evolution of the coulombic efficiency between electrolytes remains unclear as it could be due to the formation of a more efficient SEI at the K surface or at the Sb electrode surface or at both electrodes surface. In any case, these results clearly indicate that the search for efficient electrolytes for KIBs must be carried out using full cells if one wants to obtain meaningful result. Otherwise, developing efficient protection of the K metal would be of great importance. Overall, the results presented here will also more likely benefit to the development of other emerging Na, Mg-ion cell chemistries.

ASSOCIATED CONTENT

Supporting Information. Figure S1 provides the discharge/charge capacities and coulombic efficiency for 25 cycles for Sb/K coin cells filled with 0.8M KPF_6 EC:DEC and 0.8M KFSI EC:DEC. Figure S2 shows the chromatograms of the different electrolytes after storage for 3 weeks at 25°C in coin cells without and with K metal. Figure S3 and S4 shows the Carbon 1s - Potassium 2p and b) Oxygen 1s - Antimony 3d XPS core spectra of the fresh Sb electrode and Sb electrodes after storage for 3 weeks in coin cells without K metal (Figure S3) and with K metal (Figure S4) for the different electrolytes as indicated.

AUTHOR INFORMATION

Corresponding Author

*lenaic.madec@univ-pau.fr

REFERENCES

(1) Su, D.; McDonagh, A.; Qiao, S. Z.; Wang, G. High-Capacity Aqueous Potassium-Ion Batteries for Large-Scale Energy Storage. *Adv. Mater.* **2017**, *29* (1), 1–8.

(2) Matsuura, N.; Umemoto, K.; Takeuchi, Z. Standard Potentials of Alkali Metals, Silver, and Thallium Metal/Ion Couples in *N* , *N* ′-Dimethylformamide, Dimethyl Sulfoxide, and Propylene Carbonate. *Bulletin of the Chemical Society of Japan*. 1974, pp 813–817.

(3) Shannon, R. D. Revised Effective Ionic Radii and Systematic Studies of Interatomic Distances in Halides and Chalcogenides. *Acta Crystallogr* **1976**, *A32*, 751–767.

(4) Okoshi, M.; Yamada, Y.; Komaba, S.; Yamada, A.; Nakai, H. Theoretical Analysis of Interactions between Potassium Ions and Organic Electrolyte Solvents: A Comparison with

Lithium, Sodium, and Magnesium Ions. *J. Electrochem. Soc.* **2017**, *164* (2), A54–A60.

(5) Wu, X.; Leonard, D. P.; Ji, X. Emerging Non-Aqueous Potassium-Ion Batteries: Challenges and Opportunities. *Chem. Mater.* **2017**, *29* (12), 5031–5042.

(6) Zou, X.; Xiong, P.; Zhao, J.; Hu, J.; Liu, Z.; Xu, Y. Recent Research Progress in Non-Aqueous Potassium-Ion Batteries. *Phys. Chem. Chem. Phys.* **2017**, *19*, 26495–26506.

(7) Zhang, Q.; Mao, J.; Pang, W. K.; Zheng, T.; Sencadas, V.; Chen, Y.; Liu, Y.; Guo, Z. Boosting the Potassium Storage Performance of Alloy-Based Anode Materials via Electrolyte Salt Chemistry. *Adv. Energy Mater.* **2018**, *1703288*.

(8) Jiang, X.; Zhang, T.; Yang, L.; Li, G.; Lee, J. Y. A Fe/Mn-Based Prussian Blue Analogue as a K-Rich Cathode Material for Potassium-Ion Batteries. *ChemElectroChem* **2017**, *4* (9), 2237–2242.

(9) Peled, E. The Electrochemical Behavior of Alkali and Alkaline Earth Metals in Nonaqueous Battery Systems-- The Solid Electrolyte Interphase Model. *J. Electrochem. Soc.* **1979**, *126* (12), 2047–2051.

(10) Lei, K.; Li, F.; Mu, C.; Wang, J.; Zhao, Q.; Chen, C.; Chen, J. High K-Storage Performance Based on the Synergy of Dipotassium Terephthalate and Ether-Based Electrolytes. *Energy Environ. Sci.* **2017**, *10* (2), 552–557.

(11) Vaalma, C.; Giffin, G. A.; Buchholz, D.; Passerini, S. Non-Aqueous K-Ion Battery Based on Layered $K_{0.3}MnO_2$ and Hard Carbon/Carbon Black. *J. Electrochem. Soc.* **2016**, *163* (7), A1295–A1299.

(12) Lei, K.; Wang, C.; Liu, L.; Luo, Y.; Mu, C.; Li, F.; Chen, J. A Porous Network of Bismuth Used as the Anode Material for High-Energy-Density Potassium-Ion Batteries. *Angew. Chemie - Int. Ed.* **2018**, *57* (17), 4687–4691.

(13) Xiao, N.; McCulloch, W. D.; Wu, Y. Reversible Dendrite-Free Potassium Plating and Stripping Electrochemistry for Potassium Secondary Batteries. *J. Am. Chem. Soc.* **2017**, *139* (28), 9475–9478.

(14) Sloop, S. E.; Kerr, J. B.; Kinoshita, K. The Role of Li-Ion Battery Electrolyte Reactivity in Performance Decline and Self-Discharge. *J. Power Sources* **2003**, *119–121*, 330–337.

(15) Burns, J. C.; Kassam, A.; Sinha, N. N.; Downie, L. E.; Solnickova, L.; Way, B. M.; Dahn, J. R. Predicting and Extending the Lifetime of Li-Ion Batteries. *J. Electrochem. Soc.* **2013**, *160* (9), A1451–A1456.

(16) Metzger, M.; Strehle, B.; Solchenbach, S.; Gasteiger, H. A. Origin of H 2 Evolution in LIBs: H 2 O Reduction vs. Electrolyte Oxidation. *J. Electrochem. Soc.* **2016**, *163* (5), A798–A809.

(17) Petibon, R.; Madec, L.; Rotermund, L. M.; Dahn, J. R. Study of the Consumption of the Additive Prop-1-Ene-1,3-Sultone in Li[Ni0.33Mn0.33Co0.33]O2/graphite Pouch Cells and Evidence of Positive-Negative Electrode Interaction. *J. Power Sources* **2016**, *313*, 152–163.

(18) Xiong, D. J.; Petibon, R.; Nie, M.; Ma, L.; Xia, J.; Dahn, J. R. Interactions between Positive and Negative Electrodes in Li-Ion Cells Operated at High Temperature and High Voltage. *J. Electrochem. Soc.* **2016**, *163* (3), A546–A551.

(19) Madec, L.; Ellis, L. D. Exploring Interactions between Electrodes in Li[NixMnyCo1-xy]O2/Graphite Cells through Electrode/Electrolyte Interfaces Analysis. *J. Electrochem. Soc.* **2017**, *164* (14), A3718–A3726.

(20) Madec, L.; Martinez, H. Impact of the Metal Electrode Size in Half-Cells Studies: Example of graphite/Li Coin Cells. *Electrochem. commun.* **2018**, *90* (April), 61–64.

(21) Shirley, D. A. High-Resolution X-Ray Photoemission Spectrum of the Valence Bands of Gold. *Phys. Rev. B* **1972**, *5* (12), 4709–4714.

(22) McCulloch, W. D.; Ren, X.; Yu, M.; Huang, Z.; Wu, Y. Potassium-Ion Oxygen Battery Based on a High Capacity Antimony Anode. *ACS Appl. Mater. Interfaces* **2015**, *7* (47), 26158–26166.

(23) Madec, L.; Ma, L.; Nelson, K. J.; Petibon, R.; Sun, J.-P.; Hill, I. G.; Dahn, J. R. The Effects of a Ternary Electrolyte Additive System on the Electrode/Electrolyte Interfaces in High Voltage Li-Ion Cells. *J. Electrochem. Soc.* **2016**, *163* (6), A1001–A1009.

(24) Pantea, D.; Darmstadt, H.; Kaliaguine, S.; Sümmchen, L.; Roy, C. Electrical Conductivity of Thermal Carbon Blacks. *Carbon N. Y.* **2001**, *39* (8), 1147–1158.

(25) Pantea, D.; Darmstadt, H.; Kaliaguine, S.; Roy, C. Electrical Conductivity of Conductive Carbon Blacks: Influence of Surface Chemistry and Topology. *Appl. Surf. Sci.* **2003**, *217* (1–4), 181–193.

(26) Ouatani, L. El; Dedryvère, R.; Siret, C.; Biensan, P.; Reynaud, S.; Iratçabal, P.; Gonbeau, D. The Effect of Vinylene Carbonate Additive on Surface Film Formation on Both Electrodes in Li-Ion Batteries. *J. Electrochem. Soc.* **2009**, *156* (2), A103–A113.

(27) Darwiche, A.; Bodenes, L.; Madec, L.; Monconduit, L.; Martinez, H. Impact of the Salts and Solvents on the SEI Formation in Sb/Na Batteries: An XPS Analysis. *Electrochim. Acta* **2016**, *207*, 284–292.

(28) Madec, L.; Xia, J.; Petibon, R.; Nelson, K. J.; Sun, J.-P.; Hill, I. G.; Dahn, J. R. Effect of Sulfate Electrolyte Additives on LiNi1/3Mn1/3Co1/3O2/Graphite Pouch Cell Lifetime: Correlation between XPS Surface Studies and Electrochemical Test Results. *J. Phys. Chem. C* **2014**, *118*, 29608–29622.

Table of Contents graphic